Technical Physics, Vol. 47, No. 9, 2002, pp. 1152–1157. Translated from Zhurnal Tekhnicheskoĭ Fiziki, Vol. 72, No. 9, 2002, pp. 87–92.

OPTICS,
QUANTUM ELECTRONICS

1-THz Low-Noise SIS Mixer with a Double-Dipole Antenna

S. V. Shitov*, A. V. Markov*, B. D. Jackson, A. M. Baryshev**, N. N. Iosad***, J.-R. Gao***, and T. M. Klapwijk*****

** Institute of Radio Engineering and Electronics, Russian Academy of Sciences, Mokhovaya ul. 11, Moscow, 101999 Russia*

e-mail: Sergey@hitech.cplire.ru

*** National Institute for Space Research of the Netherlands (SRON), Groningen, the Netherlands*

**** Delft University of Technology (DIMES), Delft, the Netherlands*

Received January 30, 2002

Abstract—A quasi-optical mixer containing two Nb/Al/AlO$_x$/Nb superconducting tunnel junctions integrated into a NbTiN/SiO$_2$/Al microstrip line is studied experimentally in the 800–1000 GHz frequency range. The mixer is developed as an optional front end of the heterodyne receiver operating in frequency band 3 or 4 and incorporated into the HIFI module of the Herschel space-borne telescope. The double-dipole antenna of the mixer is made of NbTiN and Al films; the quarter-wavelength reflector, of a Nb film. The mixer is optimized for the IF band of 4–8 GHz. The double-sideband noise temperature T_{RX} measured at 935 GHz is 250 K at a mixer temperature of 2 K and an IF of 1.5 GHz. Within 850–1000 GHz, T_{RX} remains below 350 K. The antenna pattern is symmetrical with a sidelobe level below –16 dB. *© 2002 MAIK "Nauka/Interperiodica".*

INTRODUCTION

Low-noise heterodyne receivers of the terahertz range are necessary for designing high-efficiency space-borne telescopes, which are being developed for submillimeter spectral astronomy, for example, for the HIFI [1]. Upon tackling the problem of designing a high-sensitivity 1-THz receiver, it is reasonable to analyze the key parameters of superconductor–insulator–superconductor (SIS) mixers built on tunnel junctions.

Nb/Al/AlO$_x$/Nb tunnel-junction mixers are known as low-noise heterodyne converters. Their noise temperature on the order of hf/k_B (where h, f, and k_B are the Planck constant, frequency, and Boltzmann constant, respectively) [2] is limited by quantum fluctuations. Such mixers have been studied experimentally at 30–1500 GHz, and their noise temperature has been estimated at about (2–3)hf/k_B at frequencies below 680 GHz (the niobium gap frequency [3, 4]). Above this value, the sensitivity decreases rapidly primarily because of increased losses in niobium tuning circuits. Theoretically, the frequency range of a niobium-based SIS heterodyne converter is limited by the doubled niobium gap frequency, i.e., approximately by 1300 GHz [5]. This is because the conversion efficiency is associated with the nonlinear tunnel current of quasi-particles in SIS junction and thus does not depend directly on losses in the feeding circuits.

Designing a wide-band SIS mixer that would cover a substantial part of the subterahertz range is a challenge, since the capacitance per unit area C of an SIS junction is high. Accordingly, the loaded Q of the circuit is also high (typically about 10 at 1 THz). The high value of Q poses at least two problems: the bandwidth narrows and the losses increase. The real part of the microwave impedance of a superconducting film [6] raises the loss in proportion to the current density squared, i.e., to Q^2. Theoretically, the system's Q factor can be lowered by reducing the resistivity of the tunnel barrier, i.e., by increasing J_c. Unfortunately, this is difficult to do in practice, because the $I–V$ characteristic of the SIS junction degrades when J_c > 10–15 kA/cm^2 [7]. Another possibility of decreasing the microwave loss is to reduce the SIS junction area, which also lowers the current density in the feeding circuits. Thus, it is clear that, in general, quantum-sensitive SIS mixers are difficult to design for the frequency range where the loss in the feeding circuits is high. That is why, along with efforts in minimizing the high-frequency loss by increasing the tunnel current density and shrinking SIS junctions, advanced designs of low-loss tuning circuits based on novel materials [8–12] are of great importance for developing a terahertz-range quantum-sensitive mixer.

The capacitance of an SIS junction together with that of the integrated tuning circuits may hamper the matching of the mixer's output at the IF due to the high dynamic resistance of the junction. Under operating conditions, this resistance may be within 0.2–1.0 kΩ and even become negative [2], which leads to a high Q of the mixer's output, especially at high IFs. The problem of wide-band matching the mixer's output can be solved by decreasing the capacitance of all tuning and connecting circuits and applying a special matching transformer.

A high-frequency signal can be fed to the SIS mixer by two basic ways: through a rectangular waveguide or with the help of a quasi-optical antenna integrated with the SIS junction. The problems mentioned above are common to both designs. Specific problems may arise in fabricating precision mechanical parts of waveguide mixers. For example, the cross section of a single-mode terahertz waveguide is as small as 120×240 μm, which means that other parts such as a scalar horn, tuning pistons, a chip mounting channel, etc. must be fabricated with a micrometer precision. Auxiliary stages of chip preparation (especially dicing and grinding), as well as the assembling of a waveguide mixer, are also critical operations.

Unlike waveguide mixers, quasi-optical mixers can be fabricated on relatively large and easy-to-handle substrates, which are a part of the optical system. The parameters of these mixers depend primarily on the photolithography resolution, which is several fractions of a micron. It should be noted that the pattern of the antenna–lens system is defined by both the quality of the microwave lens and the accuracy of placing the antenna on the optical axis of the lens [13, 14]. The theoretical level of the first sidelobe of integrated lens antennas, which are most widely used, is about –18 dB, that is, slightly higher (worse) than that of scalar horns used with waveguide mixers. However, this value is adequate for most applications.

Double-slot and double-dipole antennas are widely used in planar receivers [10, 15–18]. When incorporated into an integrated lens antenna, these have similar patterns and close values of impedance. An advantage of a slot antenna is its wide ground plane, which can accommodate comparatively complex circuits near the antenna. At the same time, a double-dipole antenna was successfully used in a complex superconducting integrated receiver [16]. The back lobe of a slot antenna cannot be used as in the case of a dipole antenna, because the convergent reflector becomes inefficient. A double-dipole antenna is usually free of capacitive coupling elements, so that the average capacitance of the structure can be made lower, which is important when the IF is high.

The primary goal of this study was to develop and experimentally demonstrate a quasi-optical SIS mixer with an integrated lens antenna that meets the HIFI requirements for frequency bands 3 and 4 [1].

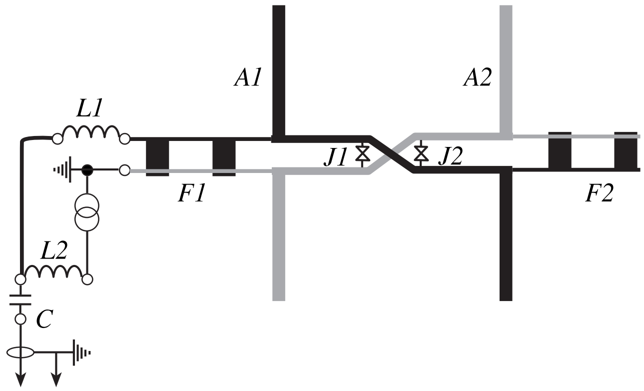

Fig. 1. Circuit diagram of a planar quasi-optical SIS mixer with a double-dipole ($A1$ and $A2$) antenna. The mixer comprises two SIS junctions ($J1$ and $J2$) that operate in antiphase and are parallel-connected in terms of IF current but series-connected in terms of microwave current. Inductance $L1 = 0.7$ nH is a tuning element at the IF output, C and $L2$ constitute the filter of the bias source, and $F1$ and $F2$ are the band-stop filters of the antenna.

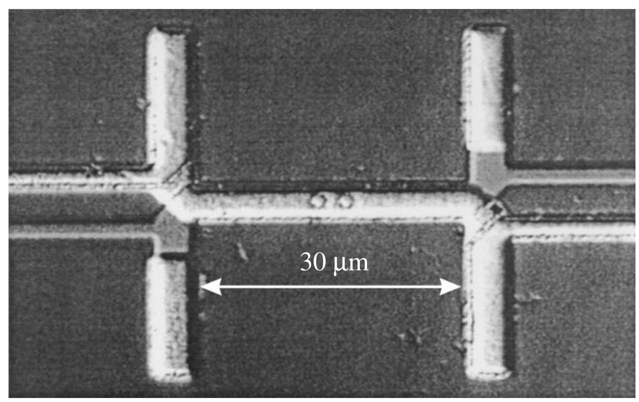

Fig. 2. SIS mixer with a double-dipole antenna on a silicon substrate. Two micron-size SIS junctions are seen at the center. Bright metal strips are aluminum; dark lines, NbTiN. The SiO_2 insulator between the electrodes is almost transparent.

GENERAL APPROACH

The structure of choice is a twin-type mixer, which contains two $Nb/Al/AlO_x/Nb$ SIS junctions connected in antiphase and a double-dipole antenna as shown in Fig. 1. This resonant structure of SIS junctions has been theoretically and experimentally shown to have a wider matching band and a lower loss than a circuit where the junction terminates a tuning microstrip line [10, 18]. The lower losses can be explained by the low density of the microwave current at the input of the impedance transformer, which is typical of twin SIS structures. To minimize the ohmic loss in the tuning circuit, we used microstrip lines made of NbTiN alloy, for which the superconductor critical temperature is about 16 K and the gap frequency is about 1 THz [19, 20]. Theoretically, such values of the parameters can provide very low losses at this frequency. The trade-off in our design is the microstrip line on the $NbTiN/SiO_2/Al$ structure. First, the upper aluminum electrode minimizes the effect of thermal trapping and, as a consequence, eliminates the overheating of the junction, which is observed in all-NbTiN tuning circuits [19]. Second, SiO_2 is far from being the optimal underlayer for the regular growth of NbTiN films, which may cause too

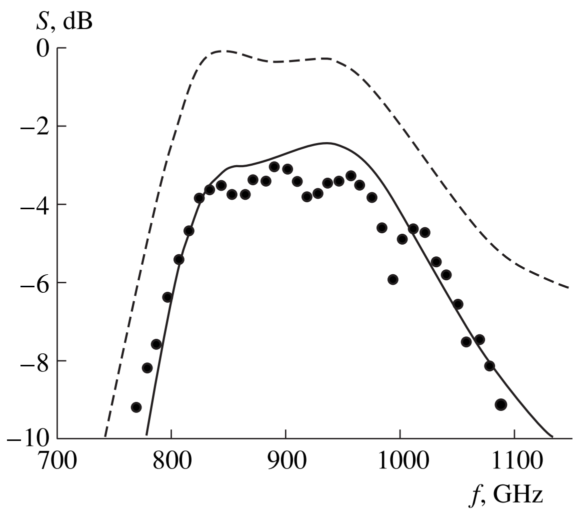

Fig. 3. Signal on the SIS junctions (circles) measured with a Fourier spectrometer and the computed values (S) (solid line). The signal level at the antenna (dashed line) is seen to be significantly higher than the signal applied to the SIS junctions because of ohmic losses in the aluminum conductors of the NbTiN/SiO_2/Al microstrip line.

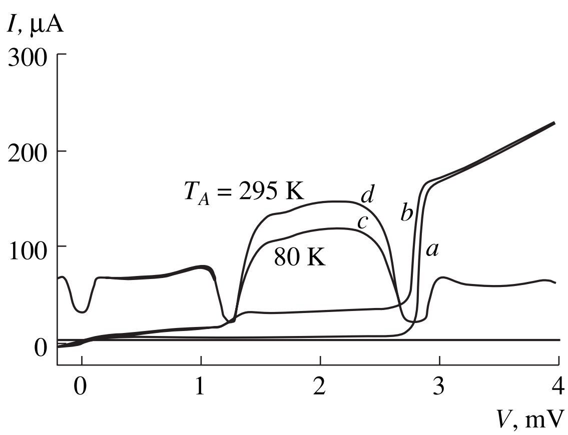

Fig. 4. (a) Autonomous and (b) pumped I–V characteristics of the SIS mixer at 955 GHz and the response to (c) "cold" and (d) "hot" antenna loads at IF = 1.5 GHz.

high losses near 1 THz due to a lower gap frequency [20].

Two identical mixers were placed 500 μm apart in the central part of a 2 × 2-mm 300-μm-thick high-resistivity silicon substrate, which was mounted on the flat back surface of a silicon elliptic lens at its focus. Such dimensions of the chip cut a 120°-wide portion from the pattern of the planar antenna, beyond which the signal is negligibly small. The second mixer on the same chip is spare. The lens diameter, 10 mm, specified both the diffraction divergence of the beam at 1 THz (about 2°) and the chip mount accuracy (about 10 μm). The IF matching circuit was designed so as to keep the reflection losses below –10 dB over the IF range of 4–8 GHz with the dynamic resistance of the mixer varying within R_d = 50–150 Ω.

DESIGN

The mixer was designed for two frequency ranges: 800–960 and 960–1120 GHz. The integrated structure was optimized individually for each of the bands separately. The double-dipole antenna shown in Fig. 2 is a scaled copy of the antenna of a 500-GHz integrated receiver [16]. The overall dimension of the antenna is 34 × 40 μm, and its elements are 4 μm wide. Initially, we assumed that the low density of the microwave current on the surface of the convergent reflector film cannot cause a significant signal loss and allows the use of almost any metal, for example, Nb. The convergent reflector chip measures 0.5 × 0.5 mm. At about 1 THz, its thickness, 22 μm, equals a quarter of the wavelength in single-crystal silicon (ε = 11.7) coated with a 200-nm-thick Nb film on one side. The antireflection coating of the microwave lens, a 46-μm-thick layer of Stycast™-1264 (ε ≈ 2.9) epoxy compound, is optimized for 960 GHz.

Two Nb/Al/AlO_x/Nb SIS junctions of area 1 μm^2 each are integrated with the antenna as shown in Figs. 1 and 2. The 3-μm-wide transmission line, which connects the antenna and two junctions placed 3.6 or 3.0 μm (depending on the frequency range) apart, is a microstrip line with a narrow (4-μm-wide) ground plane. The mixer was designed under the following assumptions. Since the configuration of the transmission line is almost symmetric, the strip and its screen can be considered interchangeable; therefore, they are connected to the antennas symmetrically. Because of the symmetry of the structure, its center can be regarded as a virtual grounding point in the middle between the two SIS junctions. Thus, the segment of the microstrip line that connects the junctions can be viewed as two independent short-circuited stubs, which are equivalent to two high-frequency tuning inductors parallel-connected to either of the SIS junctions [10].

The match of the antenna and the efficiency of transmitting the signal to the SIS junctions were computed with allowance for ohmic losses in the tuning elements. As shown in Fig. 3, the results computed are in good agreement with the experimental data obtained with a Fourier spectrometer. Our simulations assumed that the NbTiN base electrode is a perfect superconductor with a 300-nm London penetration depth. For the aluminum strip, the sheet resistance was assumed to be 0.15 Ω. Band-stop filters $F1$ and $F2$ are connected to both dipoles as shown in Fig. 1 to make the radiation pattern of the antenna system as symmetric as possible. Note that, as usual, only one filter is connected to the IF channel. The filters are designed as a periodic structure composed of quarter-wavelength sections of coplanar and microstrip lines in order to provide a high performance while retaining the small size of the device. The ohmic loss in the antenna filters turned out to be appreciable. The attenuation in the three-section filter was estimated at 6%. Basically, this value can slightly be reduced by adding sections; however, this increases the filter capacitance, making the IF matching of the mixer difficult. The curves in Fig. 3 are obtained with regard for unwanted effects, such as the inductance of the SIS junction and the inductance of current spreading around the junction window. The current spreading inductance was estimated at 0.1–0.2 pH [21].

EXPERIMENTAL RESULTS

Pilot mixers were fabricated by the process used to make waveguide devices with NbTiN and Al tuning circuits [20]. We applied conventional optical lithography. The NbTiN ground plane of the microstrip line was 300 nm thick. It was deposited at room temperature. The thickness of the SiO_2 insulator was 250 nm. The conductivity of the 400-nm-thick aluminum layer was $2 \times 10^8\ \Omega^{-1}\ m^{-1}$ at 4 K, which most likely corresponds to the anomalous limit [22]. The aluminum layer is protected against environmental attack by a 200-nm-thick SiO_2 film. A typical *I*–*V* characteristic of the pilot SIS mixer is shown in Fig. 4.

The parameters of several devices designed for frequency range 4 (960–1120 GHz) were measured in a standard vacuum cryostat with optimized IR filters with losses of 1.2 dB at 1 THz [23]. The Fourier spectrometer data suggested that the frequency response has a feature very much like the high-frequency cutoff near 1 THz. This cutoff frequency is almost independent of the SIS junction dimensions and other important tuning parameters. The double-sideband noise temperature T_{RX} for several mixers was about 500 K above 950 GHz. Since the noise temperature decreased with increasing frequency, we inferred that the device was tuned to a lower-than-optimal frequency. Eventually, a device with a center frequency slightly below 1 THz was selected. The 3-dB frequency band of this mixer determined with the Fourier spectrometer was 800–1050 GHz (Fig. 3). The responses to the change in the temperature of the matched antenna load were 1.6 dB at a mixer temperature of 4.2 K and 1.8 dB at 2 K for 935 GHz in the case of a 15-μm-thick mylar diplexer (Fig. 4). With a thinner diplexer (6 μm), the response increased to 2.1 dB, which corresponds to the double-sideband noise temperature T_{RX} = 260 K. With the correction for reflection, both diplexers gave a noise temperature of about 245 K. A water-vapor absorption line near 990 GHz is clearly seen in Fig. 5; these data were obtained at IF = 1.5 GHz.

Figure 6 shows the reflection coefficient at the IF output calculated as a function of the mixer's dynamic resistance for a total capacitance of the structure (including SIS junctions, microstrip lines, and antenna filters) of ≈0.5 pF. As follows from Fig. 6, the reflection coefficient can be kept below –10 dB for most of the

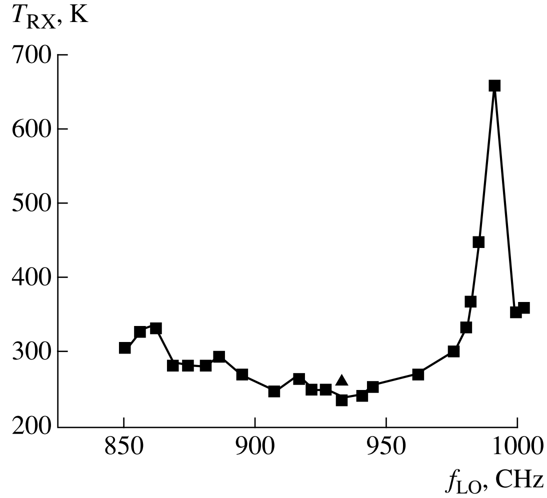

Fig. 5. Noise temperature T_{RX} in the double-sideband mode versus frequency f_{LO} of the local oscillator. The values of T_{RX} measured at about 2 K and corrected for reflection from the 15-μm-thick diplexer (squares). The triangle is a reference data point measured for the 6-μm-thick diplexer (uncorrected).

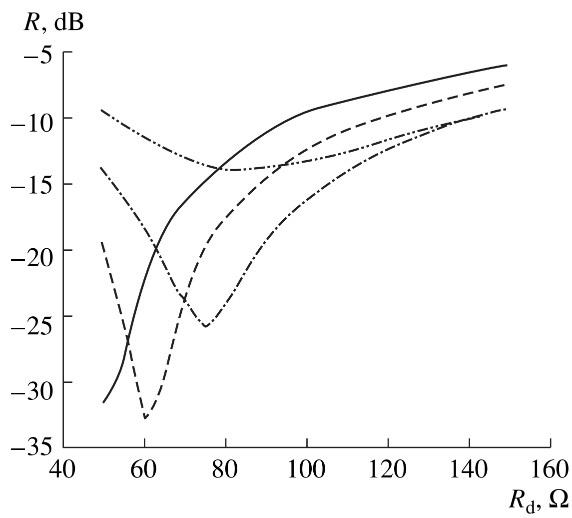

Fig. 6. Reflection losses at the IF output versus dynamic resistance of the mixer with a tuning inductance *L*1 = 0.7 nH (Fig. 1) computed at a frequency of 1.5 (solid line), 4 (dashed line), 6 (dash-and-dot line), and 8 GHz (dash-and-double-dot line).

4–8 GHz range. For a 50-Ω transmission line, this match can be achieved by using a series-connected inductance (Fig. 1). Such an inductance can be provided by bonding wires on the mixer chip. According to our calculations, the required inductance of *L* = 0.7 nH can be obtained with 1-mm-long wires that are 20–50 μm in diameter and placed 0.2 mm apart.

The antenna pattern (Fig. 7) was recorded with a narrow-beam monochromatic source with the mixer operating as a demodulator. Under such conditions, a

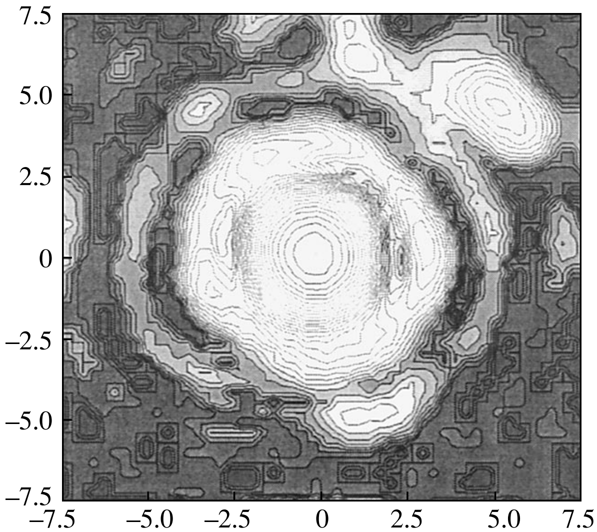

Fig. 7. Antenna pattern at 915 GHz. On both coordinate axes, the angle is plotted in degrees. The intensity isolines are spaced at 1-dB intervals. The darker the color, the lower the intensity. All sidelobes are below –16 dB. The spot in the upper right corner is most likely spurious reflections in the radiator–antenna system.

40-dB dynamic range was achieved. The receiver was turned about the phase center of the antenna. The cross section of the main lobe at 915 GHz is almost circular. The –11-dB half-width of the beam is about 1.8°; the first-order sidelobes are no higher than –16 dB. The quality of the beam remains the same up to 850 GHz. At higher frequencies, the beamwidth is smaller, as could be expected for an optical system operating in the diffraction limit. For the beamwidth to meet the HIFI requirements (F/3–F/5), we propose to supply the device with an ellipsoidal correcting mirror. The response to the cross-polarized signal component at 850 GHz is no higher than –24 dB relative to the maximum signal. This is an experimental corroboration that a lens combined with a double-dipole antenna is polarized.

CONCLUSION

A terahertz heterodyne receiver built around a quasi-optical Nb/Al/AlO_x/Nb superconducting SIS mixer integrated with a double-dipole antenna is designed, fabricated, and experimentally studied for the first time. The noise temperature of the receiver is equivalent to as little as ten photons. The device covers the 800–1000 GHz range, demonstrating a cutoff frequency of slightly above 1 THz. This result allows us to conclude that a NbTiN/SiO_2/Al tuning microstrip line deposited at room temperature may have relatively low losses at least up to 1 THz. The double-sideband noise temperature was about 250 K at 935 GHz and 360 K at 1 THz, which are the best values achieved to this point in this frequency range. The experimental results are consistent with the computed value of the effective sheet resistance of the NbTiN/SiO_2/Al microstrip line (0.1–0.2 Ω). The simulations show that a twin-type SIS mixer with a double-dipole antenna can be matched at IF in the range of 4–8 GHz. A double-dipole antenna combined with an elliptic silicon lens efficiently receives the signal in the terahertz range. The sidelobe level is below –16 dB; the cross-polar pattern is below –24 dB, which shows that a lens antenna combined with a double-dipole antenna is polarized.

ACKNOWLEDGMENTS

The authors thank Th. De Graauw and V.P. Koshelets for their encouragement and interest in this work and to D. Nguen for technical assistance.

This work was supported by the European Space Agency under the contract ESTEC no. 11653/95, the Russian State Scientific Program "Superconductivity," the Russian Foundation for Basic Research (project no. 00-02-16270), INTAS (grant no. 97-1712), and ISTC (grant no. 1199).

REFERENCES

1. http://www.sron.nl
2. J. R. Tucker and M. J. Feldman, Rev. Mod. Phys. **57**, 1055 (1985).
3. J. W. Kooi, M. Chan, B. Bumble, *et al.*, Int. J. Infrared Millim. Waves **16**, 2049 (1995).
4. A. Karpov, J. Blondel, M. Voss, *et al.*, IEEE Trans. Appl. Supercond. **9**, 4456 (1999).
5. J. A. Stern, B. Bumble, H. G. LeDuc, *et al.*, in *Proceedings of the 9th International Symposium on Space Terahertz Technology, 1998*, p. 305.
6. D. C. Mattis and J. Bardeen, Phys. Rev. **111**, 412 (1958).
7. P. Dieleman, T. M. Klapwijk, J.-R. Gao, *et al.*, IEEE Trans. Appl. Supercond. **7**, 2566 (1997).
8. H. Van de Stadt, A. M. Baryshev, P. Dieleman, *et al.*, in *Proceedings of the 6th International Symposium on Space Terahertz Technology, 1995*, p. 66.
9. V. Yu. Belitsky, S. W. Jacobsson, L. V. Filippenko, *et al.*, in *Proceedings of the 4th International Symposium on Space Terahertz Technology, 1993*, p. 538.
10. J. Zmuidzinas, H. G. LeDuc, J. A. Stern, *et al.*, IEEE Trans. Microwave Theory Tech. **42**, 698 (1994); M. Bin, M. C. Gaidis, J. Zmuidzinas, *et al.*, Appl. Phys. Lett. **68**, 1714 (1996).
11. V. Yu. Belitsky and E. L. Kollberg, J. Appl. Phys. **80**, 4741 (1996); Y. Uzawa, Z. Wang, A. Kawakami, *et al.*, in *Proceedings of the 12th International Symposium on Space Terahertz Technology, San Diego, 2001.*
12. N. N. Iosad, V. V. Roddatis, S. N. Polyakov, *et al.*, IEEE Trans. Appl. Supercond. **11**, 3970 (2001).
13. D. F. Filipovic, S. S. Gearhart, and G. M. Rebeiz, IEEE Trans. Microwave Theory Tech. **14**, 1738 (1993).
14. M. J. M. van der Vorst, P. J. I. De Maagt, and M. H. A. J. Herben, in *Proceedings of the International Symposium on Antennas (JINA'96), 1996*, p. 511;

M. J. M. van der Vorst, PILRAP, Software for Design of Integrated Lens Antennas.

15. A. Skalare, Th. De Graauw, and H. van de Stadt, Microwave Opt. Technol. Lett. **4**, 9 (1991).
16. S. V. Shitov, V. P. Koshelets, A. B. Ermakov, *et al.*, IEEE Trans. Appl. Supercond. **9**, 3773 (1999).
17. J. Zmuidzinas and H. G. LeDuc, IEEE Trans. Microwave Theory Tech. **40**, 1797 (1992).
18. S. V. Shitov, A. M. Baryshev, V. P. Koshelets, *et al.*, in *Proceedings of the 7th International Symposium on Space Terahertz Technology, 1996*, p. 525.
19. B. D. Jackson, N. N. Iosad, B. Leone, *et al.*, in *Proceedings of the 10th International Symposium on Space Terahertz Technology, 1999*, p. 144; B. Leone, B. D. Jackson, J.-R. Gao, *et al.*, Appl. Phys. Lett. **76**, 780 (2000).
20. B. D. Jackson, G. De Lange, W. M. Laauwen, *et al.*, in *Proceedings of the 11th International Symposium on Space Terahertz Technology, 2000*, p. 238.
21. M. M. Khapaev, Supercond. Sci. Technol. **9**, 729 (1996); M. Yu. Kupriyanov, private communication of the inductance calculation.
22. R. L. Kautz, J. Res. Natl. Bur. Stand. **84**, 247 (1979).
23. A. M. Baryshev, B. D. Jackson, G. De Lange, *et al.*, in *Proceedings of the 11th International Symposium on Space Terahertz Technology, 2000*, p. 129; B. D. Jackson, A. M. Baryshev, G. De Lange, *et al.*, in *Proceedings of the 12th International Symposium on Space Terahertz Technology, San Diego, 2001*.

Translated by A. Khzmalyan